

The Impact of Black Carbon Emissions from Projected Arctic Shipping on Regional Ice Transport

Xueke Li¹, Amanda Helen Lynch¹, David Anthony Bailey², and Scott R. Stephenson³

¹Brown University

²National Center for Atmospheric Research (UCAR)

³RAND Corporation

November 24, 2022

Abstract

The direct and indirect effects of global emissions of black carbon (BC) on the evolution of Arctic climate has been well documented. The significance of within-Arctic emissions of BC is less certain. In light of this, an ensemble of scenarios are developed that simulate the hypothetical diversion of 75% of current and projected shipping traffic from the Suez Canal to the Northern Sea Route (NSR). This experiment shows that BC from ships results in a small change in climate forcing that does not influence the Arctic-wide trajectory of change. However, the shift in forcing from the Suez route to the NSR not only influences regional evolution of sea ice cover, but also results in regional feedbacks that in some locations amplify (e.g. Greenland Sea) and in other locations damp (e.g. Labrador Sea) the sea ice retreat under anthropogenic climate change. The primary mechanism underlying these regional effects is a shift in circulation rather than direct thermodynamic forcing. The most significant impacts are distal from the emissions sources, which is likely to have policy implications as the expansion of industrial and transportation activities into the Arctic is considered.

1

2 **The Impact of Black Carbon Emissions from Projected Arctic Shipping on Regional**
3 **Ice Transport**

4 **Xueke Li¹, Amanda H. Lynch^{1,2}, David A. Bailey³, and Scott R. Stephenson⁴**

5 ¹Institute at Brown for Environment and Society, Brown University, Providence, RI, USA.

6 ²Department of Earth, Environmental and Planetary Sciences, Brown University, Providence, RI,
7 USA.

8 ³Climate and Global Dynamics Laboratory, National Center for Atmospheric Research, Boulder,
9 CO, USA.

10 ⁴RAND Corporation, Santa Monica, CA, USA.

11

12 Corresponding author: Xueke Li (xueke_li@brown.edu)

13 **Key Points:**

- 14 • Impact of black carbon emissions within-Arctic was quantified by re-routing 75% of
15 shipping traffic from Suez Canal to Northern Sea Route
- 16 • Feedbacks were small Arctic-wide but amplified/dampened feedbacks were observed
17 regionally primarily driven by a shift in circulation
- 18 • Largest feedback responses are distant from emission sources which has implications for
19 good governance of expanding Arctic industries

20 Abstract

21 The direct and indirect effects of global emissions of black carbon (BC) on the evolution of
22 Arctic climate has been well documented. The significance of within-Arctic emissions of BC is
23 less certain. In light of this, an ensemble of scenarios are developed that simulate the
24 hypothetical diversion of 75% of current and projected shipping traffic from the Suez Canal to
25 the Northern Sea Route (NSR). This experiment shows that BC from ships results in a small
26 change in climate forcing that does not influence the Arctic-wide trajectory of change. However,
27 the shift in forcing from the Suez route to the NSR not only influences regional evolution of sea
28 ice cover, but also results in regional feedbacks that in some locations amplify (e.g. Greenland
29 Sea) and in other locations damp (e.g. Labrador Sea) the sea ice retreat under anthropogenic
30 climate change. The primary mechanism underlying these regional effects is a shift in circulation
31 rather than direct thermodynamic forcing. The most significant impacts are distal from the
32 emissions sources, which is likely to have policy implications as the expansion of industrial and
33 transportation activities into the Arctic is considered.

34 1 Introduction

35 Investors and communities alike are planning for the possible regime shift in Arctic
36 shipping driven by receding ice, lower fuel prices, and industry consolidation [Duarte *et al.*,
37 2012; Goldstein *et al.*, 2018]. This shift has the potential, as yet unrealized, to make the
38 transpolar shipping route at least seasonally competitive with the Suez Canal [Buixadé Farré *et*
39 *al.*, 2014; Meng *et al.*, 2017; Ng *et al.*, 2018; Theocharis *et al.*, 2018]. Although the economic
40 viability of transit shipping along such Arctic routes remains under considerable debate
41 [Hildebrand and Brigham, 2018; Lasserre, 2014], ship traffic continues to increase due to
42 Russian cabotage¹ [Gunnarson, 2013], fish stock migrations, and increased tourism [Miller *et al.*,
43 2020; Stewart *et al.*, 2007].

44 Black carbon (hereinafter referred to as BC) deposition on Arctic sea ice has been posited
45 as one explanatory factor in observed rapid Arctic sea ice retreat [Ramanathan and Carmichael,
46 2008]. BC aerosols from sources including diesel engines, industrial processes and biomass
47 burning absorb strongly across visible and ultraviolet wavelengths. As a result, it can influence
48 Arctic temperatures and the extent of ice and snow cover by (i) directly absorbing solar
49 radiation; (ii) acting as nuclei to form cloud drops and ice crystals, indirectly influencing cloud
50 albedo via modifying the microphysical properties and lifetime of clouds [Haywood and
51 Boucher, 2000; Ramanathan and Carmichael, 2008]; and (iii) reducing ice and snow albedo
52 after deposition [Flanner *et al.*, 2009; Ryan *et al.*, 2018; Warren, 1982]. Previous studies suggest
53 a measured decrease in Arctic albedo of 1.5 – 3.0% caused by snow and ice darkening from BC
54 from all combustion sources, onshore and offshore [Bond *et al.*, 2013; Hansen and Nazarenko,
55 2004].

56 BC interactions and feedbacks are poorly constrained. For example, freshly emitted BC
57 particles are generally hydrophobic and cannot serve as cloud condensation nuclei (CCN).
58 Through microphysical aging processes, these carbonaceous particles gradually become
59 hydrophilic on timescales that are highly variable [Fierce *et al.*, 2015]. These particles have a
60 shorter average atmospheric residence time due to a high wet scavenging efficiency [von

¹ Cabotage in this paper, following Gunnarsson [2013], is defined as domestic port-to-port transport by both domestic and foreign carriers.

61 *Schneidmesser et al.*, 2015]. The uncertainty in atmospheric residence time of BC is particularly
62 evident in estimates of the distance from ship stacks to deposition. Given the complex web of
63 uncertain processes, ranging from changes in albedo upon deposition, changes in snow
64 metamorphism, phase partitioning in clouds, and cloud distribution properties, *Bond et al.* [2013]
65 suggest that BC has an overall positive radiative forcing, accounting for direct and indirect
66 effects, of $+1.1 \text{ Wm}^{-2}$ with 90% uncertainty bounds of $+0.17$ to $+2.1 \text{ Wm}^{-2}$. The direct radiative
67 effect, globally averaged for the industrial era, is estimated at $+0.71 \text{ Wm}^{-2}$ with 90% uncertainty
68 bounds of $+0.08$ to $+1.27 \text{ Wm}^{-2}$.

69 Maritime transport utilizing heavy fuel oil (HFO) contributes to BC emissions in the
70 Arctic via incomplete combustion [*Corbett et al.*, 2010; *Wu et al.*, 2018]. Unlike BC transported
71 to the Arctic from sub-Arctic terrestrial sources, BC emitted in the Arctic is more likely to
72 remain at low altitudes, due to the typically strong surface inversion, particularly in the winter
73 months. It has been posited that this has the potential to cause Arctic surface temperature to be
74 nearly five times more sensitive to BC emitted within the Arctic than to emissions from lower
75 latitudes, even though these emissions are much smaller in magnitude [*Sand et al.*, 2013a; *Sand*
76 *et al.*, 2016]. It is unclear, however, how the frequency of surface inversions will change in the
77 coming century [*Medeiros et al.*, 2011].

78 As a result of this potential sensitivity, studies have considered whether ship emissions of
79 BC and other particulates will amplify or damp sea ice extent and snow cover feedbacks.
80 Amplification of snow- and ice-albedo feedbacks can occur by deposition lowering the high
81 albedo of ice and snow [*Browse et al.*, 2013; *Corbett et al.*, 2010; *Ødemark et al.*, 2012; *Sand et*
82 *al.*, 2016]. Damping of these feedbacks can occur through indirect effects on clouds; for
83 example, *Stephenson et al.* [2018] find an increase in the formation of clouds with high liquid
84 water content could cause cooling relative to the shipping-free Arctic. All of these studies come
85 with the caveat that BC emissions from Arctic shipping are small compared to those from the
86 terrestrial sub-Arctic. These emissions may be reduced further in the context of a switch from
87 HFO to low-sulfur diesel fuel or LNG and the reduced need for icebreakers, but this significance
88 may increase as BC emissions from industry are reduced. Adding complexity to this issue, the
89 use of low-sulphur fuels has been linked with a possible 85 percent increase in BC emissions
90 [*DNV*, 2020]. We are seeking to understand the additional forcing of Arctic shipping-related BC,
91 and in particular whether it constitutes a feedback of significance in the evolving system.

92 **2 Data and methods**

93 **2.1 Climate Model Configuration**

94 To quantify climate feedbacks of BC, we use the newly released Community Earth
95 System Model version 2 (CESM2) at approximately 1° horizontal resolution with 32 vertical
96 layers. CESM2 is a fully coupled earth system model that provides state-of-the-art simulations of
97 climate. It contains seven prognostic model components (CAM6/WACCM6, CLM5, CISM2,
98 POP2, CICE5, MOSART, and WW3) to comprehensively represent interactions among
99 atmosphere, land, land-ice, ocean, and sea ice [*Danabasoglu et al.*, 2020].

100 CAM6 improves upon its previous version by including a unified turbulence scheme
101 [*Golaz et al.*, 2002], adopting an updated Morrison–Gettelman cloud microphysics scheme
102 (MG2) [*Gettelman and Morrison*, 2015], and applying a new scheme to calculate subgrid
103 orographic drag [*Beljaars et al.*, 2004]. Notably, CAM6 treats aerosols using a four-mode

104 version of Modal Aerosol Model (MAM4) [Liu *et al.*, 2016]. That is, apart from Aitken,
105 accumulation, and coarse modes preserved in the three-mode version (MAM3) [Liu *et al.*, 2012],
106 an additional primary carbon mode is included in MAM4 to reside freshly emitted particulate
107 organic matter (POM) and BC particles. This strategy allows for the conversion of particles from
108 hydrophobic to hydrophilic. Compared to simulations with MAM3 that combine the primary
109 carbon mode with the accumulation mode, which as a consequence, enhances wet removal of
110 BC, the treatment of separating the primary carbon mode from the accumulation mode in MAM4
111 increases near-surface BC concentrations in the polar regions by a factor of 2 to 10 [Liu *et al.*,
112 2016].

113 In addition, the CESM large ensemble (CESM1-LENS, Kay *et al.* 2015) is used as a kind
114 of proxy testbed [Deser *et al.*, 2020] to provide a more nuanced assessment of uncertainties
115 arising from internal variability. The Large Ensemble Project provides 40 ensemble members
116 performed with 1° resolution of fully-coupled CESM1 under RCP 8.5 from 2006-2100. As is
117 standard practice, the slightly varying initial condition leads to an ensemble spread solely due to
118 the model's internal climate variability [Kay *et al.*, 2015]. While this is not the model
119 implementation used here, it can provide guidance as to the spread that might be expected in
120 model responses in the present application. It should be noted that at the time of submission, all
121 of the required variables from the CESM2 implementation of this large ensemble were not
122 available.

123 2.2 Shipping emissions scenarios

124 Two sets of climate simulations with the CESM2 from 2015 to 2065 are performed. In
125 the control experiment, projected monthly BC emissions from simulated trans-Arctic voyages are
126 injected into the atmosphere along with BC emissions from Peters *et al.* [2011] and other
127 emissions inventories from IPCC AR5 [Lamarque *et al.*, 2010] based on the Shared
128 Socioeconomic Pathways (SSPs) 5 under the Representative Concentration Pathway (RCP) 8.5
129 scenario (O'Neill *et al.*, 2016, hereinafter referred to as SSP5-8.5). BC emitted from Arctic
130 shipping is injected in the primary carbon mode of CAM6.

131 Small errors in the existing CMIP6 SSP5-8.5 scenario forcing (Figure 1(a)) were
132 corrected to create a new control experiment rather than using the standard CMIP6 scenario. The
133 main issues with the original SSP5-8.5 data are as follows. First, BC emissions in the standard
134 scenario assume that the NSR is navigable all year round regardless of ice cover, when in reality,
135 Arctic voyages are heavily concentrated in the peak months of July through October. We
136 therefore limited shipping emissions to those months in which the NSR was technically
137 accessible following the method of Stephenson *et al.* [2018], in order to reflect the seasonal cycle
138 of Arctic shipping traffic. Second, there are interpolation artifacts in the standard scenario that
139 are evident year round near the North Pole, which we have termed the “Santa Claus effect”;
140 these were removed. Third, the HFO ban was implemented from 2020 in the standard scenario,
141 but it is not yet in force. In October 2020, the IMO will vote on whether to approve a
142 recommendation to ban the use and carriage of HFO in the Arctic by July 1, 2029 for Arctic
143 country-flagged vessels operating in domestic waters, and by July 1, 2024 for all other voyages
144 [Humpert, 2020]. Given that Russian vessels operating along the NSR are exempted from the
145 shorter timeframe, approval by all Arctic states appears likely. Nevertheless, in the SSP5-8.5
146 forcing, the BC emissions are assumed to rise until 2020 and then begin to drop after this point,
147 likely due to other treaties and not related to the HFO ban [O'Neill *et al.*, 2014]. To address this

148 complexity, the BC emissions in the new control simulation are modified as shown in Figure
149 1(b).

150 With the recent fall in oil prices, reasons to utilize the NSR for transit shipping have been
151 less compelling in the near term. International transit shipping utilizing the entire NSR
152 comprised less than 1% of all voyages from 2016-2018 [B. Gunnarson, *personal communication*,
153 2020]. These transits were primarily associated with demonstration voyages and the
154 repositioning of vessels. In contrast, cabotage along the Russian Arctic coast comprised 88% of
155 the total voyages on average over the same period, with monthly peaks of at least 250 voyages
156 from July to October, and up to 400 voyages in September in some years. Thus, emissions
157 associated with NSR transit shipping are a small fraction of the total BC load associated with
158 Arctic shipping at present. Furthermore, the BC load in the Arctic is comprised primarily of sub-
159 Arctic terrestrial sources [Law and Stohl, 2007; Shindell *et al.*, 2008]. In this uncertain context,
160 to unambiguously characterize the climatic response to a postulated highly active route, a large
161 perturbation was designed. The experiment is thus designated “big kick”. Specifically, this
162 approach lays the groundwork for understanding better what useful information might be gleaned
163 from climate simulations of the impacts of NSR shipping in general, and where greater precision
164 is likely to be most effective. In that spirit, an ensemble of integrations is conducted that re-
165 routes 75% of BC emissions from current and projected Suez Canal traffic [Gidden *et al.*, 2019]
166 to the Arctic, at equal 0.5-degree intervals along a route from the Bering Strait to Rotterdam
167 (Figure 1(c)). Each of the ensemble members was performed with the “big kick” emissions, and
168 a small perturbation to the surface air temperature to create internal variability. While four
169 ensemble members is small, this should be sufficient to detect a signal in atmospheric circulation
170 and sea ice responses, as described in Deser *et al.* [2012].

171 2.3 Quantifying feedback gain

172 An important target for this analysis is to reach an understanding of the potential for BC
173 load to amplify or damp greenhouse gas feedback effects, as opposed to simply quantifying the
174 additional forcing (both positive and negative) that BC imposes on the system. BC has potential
175 for impacts that both amplify (through albedo reduction, Hansen and Nazarenko, 2004) and
176 damp (through increases in cloud liquid water content, Stephenson *et al.*, 2018) the response to
177 climate change. This is addressed through a feedback gain calculation following Dufresne and
178 Bony [2008] based on the simple planetary energy balance response to a change in radiative
179 forcing ΔR , viz.,

$$180 \quad \Delta T = \frac{\Delta F_{TOA}^{rad} - \Delta R}{\lambda} \quad (1)$$

181 The total feedback effect can be divided into:

$$182 \quad \lambda = \lambda_0 + \lambda_w + \lambda_{LR} + \lambda_c + \lambda_\alpha \quad (2)$$

183 where λ_0 , λ_w , λ_{LR} , λ_c , and λ_α are feedback parameters of Planck, water vapor, lapse rate, cloud,
184 and albedo, respectively. To this set, we add a hypothesized BC feedback parameter. Using this
185 we can compare the basic equilibrium response to the observed temperature response, for
186 example, by defining a feedback gain variable:

$$187 \quad \Delta T = \frac{1}{1-g} \Delta T_E \quad (3)$$

188 in which $g = \sum_{x \neq 0} g_x$, and $g_x = -\frac{\lambda_x}{\lambda_0}$. Thus, we can calculate the feedback gain due to the
 189 change in BC forcing between the control and “big kick” experiments by

$$190 \quad \Delta T_{65-15, "big\ kick"} = \frac{1}{1-g_{BC}} \Delta T_{65-15, control} \quad (4)$$

191 A similar procedure can be followed for ice volume and area. We acknowledge that our
 192 experiments are not in equilibrium, but nevertheless this is a useful measure that allows the
 193 integration of multiple interacting effects into a single metric. This serves to direct attention to
 194 more detailed analysis.

195 For analysis of the whole Arctic Ocean and its sub-regions, we define the Arctic
 196 following *Parkinson and Cavalieri* [2008] (thumbnail image shown in Figure 3(a)) with
 197 constituent sub-regions demarcating the Labrador Sea, the Greenland Sea, the Barents and Kara
 198 Seas, the Siberian Sea, the Beaufort Sea, the Central Arctic, the Arctic Ocean (including the
 199 Siberian Sea, the Beaufort Sea, and the Central Arctic, not shown), the Bering Sea, Seas of
 200 Okhotsk, the Canadian Archipelago, and Hudson Bay, abbreviated as Lab, GIN, Bar, Sib, Beau,
 201 CArc, ArcOc, Bering, Okhotsk, CAArch, and Hudson, respectively.

202 **3 Whole Arctic Response**

203 The total response to BC over the whole Arctic - ice volume, concentration, and
 204 distribution, surface temperature, broadband albedo, cloud fraction, longwave and shortwave
 205 heating rates - is modest, in line with previous studies [*Flanner, 2013; Holland et al., 2012; Sand*
 206 *et al., 2013b*]. These are not shown, since the significant differences (even at the 90%
 207 significance level) are very small. An indication of these differences is summarized in Table 1, in
 208 the form of linear trends for the last thirty years of the integrations (2035-2065) for the control
 209 experiment and the “big kick” ensemble mean. Based on these trends, it could be argued that the
 210 ice volume across the whole Arctic diminishes slightly more rapidly and the temperature
 211 increases slightly more in the ensemble mean compared to the control, as the presence of
 212 additional BC load in the atmosphere does result in the expected physical responses. But as is
 213 readily apparent, in the context of high interannual variability in this system, these results in
 214 aggregate are not statistically significant. More detail can be seen for example in Figure 2, which
 215 shows the time series of ice volume differences from each season, averaged across the ensemble
 216 members, expressed as a Z-score. This behavior is quite representative of individual ensemble
 217 member results in every season, and of other measures such as surface temperature and
 218 longwave heating rate. As is readily apparent, on an Arctic-wide basis, the rate of ice loss does
 219 not accelerate in the “big kick” experiment ensemble relative to the control. Thus, it is apparent
 220 that there is no net amplification (nor a damping) of the response that is sufficient to set up an
 221 additional feedback in the whole Arctic system.

222 This conclusion is reflected most efficiently in the calculation of the feedback gain
 223 parameter. In order to set bounds for significance in the feedback gain parameter, the CESM1-
 224 LENS ensemble members were compared pairwise (Figure 3(a)). The gain calculation is shown
 225 for the entire Arctic at the left of the figure, as well as being disaggregated into each the Arctic
 226 Seas. The median feedback for the whole Arctic is 0.00 with standard deviation of 0.21 for
 227 surface temperature, 0.21 for ice concentration and 0.20 for ice volume. The shading corresponds
 228 to the probability that the feedback gain magnitude would have been evident through internal
 229 system variability alone. This figure shows the potential for large feedback gain values evident

230 particularly in the Barents and Bering Seas generated by internal variability in the ensemble.
231 Bringing the focus to the range more typical of the experiments being assessed here (Figure 3(b))
232 shows that - for the whole Arctic - the feedback gain in the “big kick” experiment cannot be
233 considered to be significant for surface temperature, aggregate ice concentration or ice volume
234 per unit area. As a result, it can be concluded that this experiment confirms previous research
235 indicating that Arctic shipping, while having the potential to perhaps slightly influence the
236 trajectory of Arctic sea ice retreat, does not induce additional Arctic-wide feedbacks.

237 **4 Regional response**

238 The same cannot be said, however, when disaggregating the response. Figure 3 also
239 shows the feedback gain parameter for 11 distinct regions of the Arctic. The median feedback
240 gain for the CESM1-LENS is zero for each of these regions. It is apparent that feedbacks are
241 generated in the “big kick” ensemble in some of these regions at levels that amply exceed one
242 standard deviation in the CESM1-LENS. While this cannot be a strict test of statistical
243 significance, because of the different model configurations, it can serve as a guide to model
244 responses that are likely to be outside of expectation from random chance.

245 The larger feedback gain values are negative in Baffin Bay and the Labrador and Siberian
246 Seas, strongly positive in the Bering Sea, and somewhat positive in the GIN Seas and to a lesser
247 extent the Barents/Kara Seas. The differing signs of the feedback gain in different regions
248 suggest why the Arctic-wide feedback is effectively zero. That said, even though the median is
249 zero, the variance in internally generated feedback gain in the CESM1-LENS is substantially
250 greater than one in the Bering and Barents/Kara Seas, and as a result these two regions will be
251 largely excluded from the following discussion.

252 It is particularly meaningful from a policy standpoint that the regions showing the largest
253 “significant” feedback responses are distant from the regions where the additional BC load of the
254 “big kick” experiment is largest (Figure 1). Furthermore, this suggests that the ice changes are
255 influenced, if not driven, by perturbations in ice and atmosphere dynamical effects rather than
256 albedo forcing by proximal deposition, or local cloud radiative forcing. This is borne out by, for
257 example, a comparison of the longwave and shortwave heating rates in the GIN Seas (see
258 supplementary Figure S1).

259 The sea level pressure (SLP) changes provide a useful indicator of atmospheric
260 dynamical responses to the imposed BC load. The changes are modest but systematic, and may
261 be summarized as a small but consistent tendency toward less negative indices for both the
262 Northern Annular Mode and the Arctic dipole patterns (which can be diagnosed, for example,
263 from the loadings onto EOF1 and 2 in the 1000hPa height fields, but are also apparent in the SLP
264 patterns). This effect is in the context of an enhancement in the propensity toward a negative
265 index Northern Annular Mode associated with greenhouse gas emissions that is typical of most
266 climate change scenarios [Gillett and Fyfe; 2013]. These small shifts in the circulation that act as
267 a perturbation on greenhouse gas forcing result in a reduction in the transpolar drift stream, a
268 weakening of ice evacuation from the Siberian coast toward the Beaufort Sea, and a weakening
269 of the ice exported out through the Bering Strait. All of these effects are consistent with the
270 negative feedback gain parameter in the Siberian Sea and with findings such as those of Wang *et*
271 *al.* [2009]. This is also consistent with the small but positive feedback gain in the aggregate ice
272 area in the Beaufort Sea.

273 In the spring (MAM), there is also an eastward shift of the Siberian high associated with
274 the Arctic Dipole (AD) in the ensemble mean “big kick” experiment (Figure 4). While the
275 loading onto the AD mode varies across ensemble members, all members show an increasing
276 propensity toward a positive mode in the last two decades of the simulations. This shift towards a
277 slightly positive phase of AD has been demonstrated to lead to favorable conditions for enhanced
278 ice export toward the Atlantic [*Watanabe et al.*, 2006].

279 In the summer (JJA), the SLP difference between the ensemble mean and the control
280 reveals positive values centered on the western Arctic (that is, Iceland-Greenland-Canadian
281 Archipelago-Beaufort Sea) and negative values centered on the eastern Arctic (Barents and Kara
282 Seas-Laptev Sea-Siberian Sea). This feature is also evident in the results of *Overland et al.*
283 [2012]. This persistent AD signature facilitates southerly wind flow from the Bering Strait,
284 bringing warm North Pacific waters into the Arctic Ocean, but also accelerating ice export
285 through Fram Strait [*Wang et al.*, 2009].

286 The signal in the North Atlantic is stronger, whereby the deepening of the polar low
287 storm track in the GIN Seas is apparent, in all seasons, but particularly winter (DJF) and spring
288 (MAM) (Figure 4). The impact on the ice regime in MAM is shown in Figure 5 for total,
289 dynamic, ridging and thermodynamic ice differences from “big kick” ensemble member 1 for
290 enhanced clarity (with the total MAM ice volume change for the other ensemble members shown
291 in supplementary Figure S2). The overall impact in ice volume shows a redistribution from the
292 eastern Barents and Kara Seas to the marginal ice zone in the GIN Seas. This is as a result
293 particularly of the influence of dynamical processes as shown in the difference in ice volume due
294 to ice transport and ridging (Figures 5(b) and (c)), although this is also reflected somewhat in the
295 distribution of ice growth and melt (Figure 5(d)). An enhancement of the polar low storm track
296 in all seasons apart from summer (JJA) leads to an increase in the incursion of sub-Arctic air into
297 the region, with concomitant warming in the GIN and Barents Seas. Consistent with this logic
298 are ice velocities that are generally more cyclonic in this region in the “big kick” ensemble
299 members and increased ice drift speed in the region of enhanced export. As a result, significant
300 changes in the ice regime are manifest all along the eastern Greenland coast even though this is
301 distal from the perturbation in shipping activity.

302 The negative feedback gain parameters in the Baffin Bay and Labrador Sea region are
303 also driven primarily by ice transport effects. This region, typical of Arctic projections, maintains
304 a relatively heavy seasonal ice cover throughout much of the simulation across seasons, with
305 spring (MAM) ice concentrations relatively flat at around 60% throughout the entire integration,
306 even as the region is close to ice free in fall (SON). Ice thickness decreases in every season, and
307 most rapidly in winter (DJF) and spring (MAM). Consistent signals across all ensemble members
308 yielding statistically significant differences are also evident in warming temperatures and
309 increased ice export from Baffin Bay out through the Labrador Sea. These changes in ice regime
310 are then reflected in an increase in ice associated with thermodynamic growth. The conclusion
311 based on these observations is that the modest additional warming evident in the “big kick”
312 experiment is insufficient to offset the increased growth in ice as the shift in ice drift evacuates
313 ice toward the south. A negative feedback then results in the western Greenland coastal zone.

314 This kind of integrative impact on ice cover associated with subtle shifts in circulation
315 has been documented by *Kwok* [2000]; *Maslanik et al.* [2000]; and *Rigor et al.* [2002]. These
316 dynamical mechanisms may also have profound implications for weather extremes in the mid-
317 latitude [*Cohen et al.*, 2014; *Coumou et al.*, 2018].

318 **5 Discussion**

319 The future significance of international transit shipping in the Northern Sea Route will
320 depend on numerous factors, including the interests and aspirations of Arctic nations, a
321 sustainable cargo base, the length of the navigation season, and the availability of navigational
322 support infrastructure. In this context, the effects of shipping on the climate system of the Arctic
323 are small, but in our view, not insignificant.

324 The mitigation of black carbon emissions was expected to present “a potentially valuable
325 opportunity with a very short delay between action and effect” [Grieshop *et al.*, 2009, p. 533].
326 This is particularly true for the Arctic due to the short time from emission to deposition (days to
327 weeks [Bond *et al.*, 2013; Hansen and Nazarenko, 2004]). Our findings suggest this opportunity
328 is more limited than might have been hoped. It is evident from these experiments and analyses
329 that even a large perturbation in the usage of the Northern Sea Route, with its concomitant
330 increase in black carbon emissions, is unlikely to be a significant factor in accelerating Arctic sea
331 ice loss. Indeed, these simulations did not include the impacts of sulfate aerosols that attend
332 enhancing shipping emissions, which can often yield a cooling effect [Stephenson *et al.*, 2018].
333 What is significant, however, is that these emissions do have the potential to affect regional
334 feedback processes, that the mechanism underlying these effects is largely dynamical changes in
335 the system, and that the most significant impacts are distal from the emissions themselves.
336 Importantly, it appears that an important response is via the North Atlantic storm track, which
337 has significance for operations in this busy region of the Arctic. As a result, policy-makers may
338 have an interest in knowing more precisely what level of black carbon load, regardless of source,
339 induces the observed regional changes.

340 Furthermore, the future of emissions contributions from Arctic ships - be they engaged in
341 fishing, cabotage or transit - depends on the speed of technological developments and adoptions
342 toward zero-emission fuels. The International Maritime Organization aims to halve emissions
343 from shipping by 2050, while Arctic nations may adopt more ambitious targets in their sovereign
344 seas. For example, the Norwegian Shipowners’ Association has stated a goal of halving
345 emissions by 2030, and to purchase only ships with zero-emissions technology from 2030. While
346 these are relatively minor goals in the global black carbon budget, such aspirations form an
347 important part of an overarching maritime shipping strategy.

348 **Acknowledgments**

349 This research was funded by the National Science Foundation through grant NNA/CNH-S
350 1824829: Modeling risk from variation in a coupled natural-human system at the Arctic ice edge.
351 The authors appreciate the insightful discussions with Siri Veland and Michael Goldstein on the
352 motivations for and relevance of these simulations for policy and communities. There are no
353 conflicts of interest to report for any authors on this paper, not for the colleagues we
354 acknowledge here. Previous and current CESM versions are freely available at
355 www.cesm.ucar.edu/models/cesm2/. Computing and data storage resources, including the
356 Cheyenne supercomputer (doi:10.5065/D6RX99HX), were provided by the Computational and
357 Information Systems Laboratory (CISL) at NCAR. The CESM datasets used in this study will be
358 made available upon acceptance of the manuscript from the Earth System Grid Federation
359 (ESGF) at esgf-node.llnl.gov/search/cmip6, or from the NCAR Digital Asset Services Hub
360 (DASH) at data.ucar.edu.

361 **References**

- 362 Beljaars, A. C. M., A. R. Brown, and N. Wood (2004), A new parametrization of turbulent
363 orographic form drag, *Quarterly Journal of the Royal Meteorological Society*, *130*(599), 1327-
364 1347, doi:10.1256/qj.03.73.
- 365 Bond, T. C., et al. (2013), Bounding the role of black carbon in the climate system: A scientific
366 assessment, *Journal of Geophysical Research: Atmospheres*, *118*(11), 5380-5552,
367 doi:10.1002/jgrd.50171.
- 368 Browse, J., K. S. Carslaw, A. Schmidt, and J. J. Corbett (2013), Impact of future Arctic shipping
369 on high-latitude black carbon deposition, *Geophysical Research Letters*, *40*(16), 4459-4463,
370 doi:10.1002/grl.50876.
- 371 Buixadé Farré, A., et al. (2014), Commercial Arctic shipping through the Northeast Passage:
372 routes, resources, governance, technology, and infrastructure, *Polar Geography*, *37*(4), 298-324,
373 doi:10.1080/1088937X.2014.965769.
- 374 Cohen, J., et al. (2014), Recent Arctic amplification and extreme mid-latitude weather, *Nature*
375 *Geoscience*, *7*(9), 627-637, doi:10.1038/ngeo2234.
- 376 Corbett, J. J., D. A. Lack, J. J. Winebrake, S. Harder, J. A. Silberman, and M. Gold (2010),
377 Arctic shipping emissions inventories and future scenarios, *Atmos. Chem. Phys.*, *10*(19), 9689-
378 9704, doi:10.5194/acp-10-9689-2010.
- 379 Coumou, D., G. Di Capua, S. Vavrus, L. Wang, and S. Wang (2018), The influence of Arctic
380 amplification on mid-latitude summer circulation, *Nature Communications*, *9*(1), 2959,
381 doi:10.1038/s41467-018-05256-8.
- 382 Danabasoglu, G., et al. (2020), The Community Earth System Model Version 2 (CESM2),
383 *Journal of Advances in Modeling Earth Systems*, *12*(2), e2019MS001916,
384 doi:10.1029/2019ms001916.
- 385 Deser, C., et al. (2020), Insights from Earth system model initial-condition large ensembles and
386 future prospects, *Nature Climate Change*, *10*(4), 277-286, doi:10.1038/s41558-020-0731-2.
- 387 Deser, C., A. Phillips, V. Bourdette, and H. Teng (2012), Uncertainty in climate change
388 projections: the role of internal variability, *Climate Dynamics*, *38*(3), 527-546,
389 doi:10.1007/s00382-010-0977-x.
- 390 DNV, G. (2020), Initial results of a Black Carbon measurement campaign with emphasis on the
391 impact of the fuel oil quality on Black Carbon emissions. Retrieved from
392 [https://www.euractiv.com/wp-content/uploads/sites/2/2020/01/PPR-7-8-Initial-results-of-a-
393 Black-Carbon-measurement-campaign-with-emphasis-on-the-impact-of-the...-Finland-and-
394 Germany.pdf](https://www.euractiv.com/wp-content/uploads/sites/2/2020/01/PPR-7-8-Initial-results-of-a-Black-Carbon-measurement-campaign-with-emphasis-on-the-impact-of-the...-Finland-and-Germany.pdf).
- 395 Duarte, C. M., T. M. Lenton, P. Wadhams, and P. Wassmann (2012), Abrupt climate change in
396 the Arctic, *Nature Climate Change*, *2*(2), 60-62, doi:10.1038/nclimate1386.
- 397 Dufresne, J.-L., and S. Bony (2008), An Assessment of the Primary Sources of Spread of Global
398 Warming Estimates from Coupled Atmosphere–Ocean Models, *Journal of Climate*, *21*(19),
399 5135-5144, doi:10.1175/2008jcli2239.1.

- 400 Fierce, L., N. Riemer, and T. C. Bond (2015), Explaining variance in black carbon's aging
401 timescale, *Atmos. Chem. Phys.*, *15*(6), 3173-3191, doi:10.5194/acp-15-3173-2015.
- 402 Flanner, M. G. (2013), Arctic climate sensitivity to local black carbon, *Journal of Geophysical*
403 *Research: Atmospheres*, *118*(4), 1840-1851, doi:10.1002/jgrd.50176.
- 404 Flanner, M. G., C. S. Zender, P. G. Hess, N. M. Mahowald, T. H. Painter, V. Ramanathan, and P.
405 J. Rasch (2009), Springtime warming and reduced snow cover from carbonaceous particles,
406 *Atmos. Chem. Phys.*, *9*(7), 2481-2497, doi:10.5194/acp-9-2481-2009.
- 407 Gettelman, A., and H. Morrison (2015), Advanced Two-Moment Bulk Microphysics for Global
408 Models. Part I: Off-Line Tests and Comparison with Other Schemes, *Journal of Climate*, *28*(3),
409 1268-1287, doi:10.1175/jcli-d-14-00102.1.
- 410 Gidden, M. J., et al. (2019), Global emissions pathways under different socioeconomic scenarios
411 for use in CMIP6: a dataset of harmonized emissions trajectories through the end of the century,
412 *Geosci. Model Dev.*, *12*(4), 1443-1475, doi:10.5194/gmd-12-1443-2019.
- 413 Gillett, N. P., and J. C. Fyfe (2013), Annular mode changes in the CMIP5 simulations,
414 *Geophysical Research Letters*, *40*(6), 1189-1193, doi:10.1002/grl.50249.
- 415 Golaz, J.-C., V. E. Larson, and W. R. Cotton (2002), A PDF-Based Model for Boundary Layer
416 Clouds. Part I: Method and Model Description, *Journal of the Atmospheric Sciences*, *59*(24),
417 3540-3551, doi:10.1175/1520-0469(2002)059<3540:apbmf>2.0.co;2.
- 418 Goldstein, M. A., A. H. Lynch, A. Zsom, T. Arbetter, A. Chang, and F. Fetterer (2018), The
419 step-like evolution of Arctic open water, *Scientific Reports*, *8*(1), 16902, doi:10.1038/s41598-
420 018-35064-5.
- 421 Grieshop, A. P., C. C. O. Reynolds, M. Kandlikar, and H. Dowlatabadi (2009), A black-carbon
422 mitigation wedge, *Nature Geoscience*, *2*(8), 533-534, doi:10.1038/ngeo595.
- 423 Gunnarson, B. (2013), The future of Arctic marine operations and shipping logistics, in *The*
424 *Arctic in World Affairs: A North Pacific Dialogue on the Future of the Arctic, Proceedings of the*
425 *North Pacific Arctic Conference (NPAC)*, edited by O.R. Young, J.-D. Kim, and Y.H. Kim, pp.
426 37–61, Korea Maritime Institute and East-West Center, Seoul and Honolulu.
- 427 Hansen, J., and L. Nazarenko (2004), Soot climate forcing via snow and ice albedos,
428 *Proceedings of the National Academy of Sciences of the United States of America*, *101*(2), 423-
429 428, doi:10.1073/pnas.2237157100.
- 430 Haywood, J., and O. Boucher (2000), Estimates of the direct and indirect radiative forcing due to
431 tropospheric aerosols: A review, *Reviews of Geophysics*, *38*(4), 513-543,
432 doi:10.1029/1999RG000078.
- 433 Hildebrand, L. P., and L. W. Brigham (2018), Navigating the Future: Towards Sustainable Arctic
434 Marine Operations and Shipping in a Changing Arctic, in *Sustainable Shipping in a Changing*
435 *Arctic*, edited by L. P. Hildebrand, L. W. Brigham and T. M. Johansson, pp. 429-435, Springer
436 International Publishing, Cham, doi:10.1007/978-3-319-78425-0_23.
- 437 Holland, M. M., D. A. Bailey, B. P. Briegleb, B. Light, and E. Hunke (2012), Improved Sea Ice
438 Shortwave Radiation Physics in CCSM4: The Impact of Melt Ponds and Aerosols on Arctic Sea
439 Ice, *Journal of Climate*, *25*(5), 1413-1430, doi:10.1175/jcli-d-11-00078.1.

- 440 Humpert, M. (2020). IMO moves forward with ban of Arctic HFO but exempts some vessels
441 until 2029. *High North News*, February 24. [https://www.highnorthnews.com/en/imo-moves-](https://www.highnorthnews.com/en/imo-moves-forward-ban-arctic-hfo-exempts-some-vessels-until-2029)
442 [forward-ban-arctic-hfo-exempts-some-vessels-until-2029](https://www.highnorthnews.com/en/imo-moves-forward-ban-arctic-hfo-exempts-some-vessels-until-2029)
- 443 Kay, J. E., et al. (2015), The Community Earth System Model (CESM) Large Ensemble Project:
444 A Community Resource for Studying Climate Change in the Presence of Internal Climate
445 Variability, *Bulletin of the American Meteorological Society*, 96(8), 1333-1349,
446 doi:10.1175/bams-d-13-00255.1.
- 447 Kwok, R. (2000), Recent changes in Arctic Ocean sea ice motion associated with the North
448 Atlantic Oscillation, *Geophysical Research Letters*, 27(6), 775-778, doi:10.1029/1999gl002382.
- 449 Lamarque, J. F., et al. (2010), Historical (1850–2000) gridded anthropogenic and biomass
450 burning emissions of reactive gases and aerosols: methodology and application, *Atmos. Chem.*
451 *Phys.*, 10(15), 7017-7039, doi:10.5194/acp-10-7017-2010.
- 452 Lasserre, F. (2014), Case studies of shipping along Arctic routes. Analysis and profitability
453 perspectives for the container sector, *Transportation Research Part A: Policy and Practice*, 66,
454 144-161, doi:https://doi.org/10.1016/j.tra.2014.05.005.
- 455 Law, K. S., and A. Stohl (2007), Arctic Air Pollution: Origins and Impacts, *Science*, 315(5818),
456 1537-1540, doi:10.1126/science.1137695.
- 457 Liu, X., et al. (2012), Toward a minimal representation of aerosols in climate models: description
458 and evaluation in the Community Atmosphere Model CAM5, *Geosci. Model Dev.*, 5(3), 709-
459 739, doi:10.5194/gmd-5-709-2012.
- 460 Liu, X., P. L. Ma, H. Wang, S. Tilmes, B. Singh, R. C. Easter, S. J. Ghan, and P. J. Rasch (2016),
461 Description and evaluation of a new four-mode version of the Modal Aerosol Module (MAM4)
462 within version 5.3 of the Community Atmosphere Model, *Geosci. Model Dev.*, 9(2), 505-522,
463 doi:10.5194/gmd-9-505-2016.
- 464 Maslanik, J. A., A. H. Lynch, M. C. Serreze, and W. Wu (2000), A Case Study of Regional
465 Climate Anomalies in the Arctic: Performance Requirements for a Coupled Model, *Journal of*
466 *Climate*, 13(2), 383-401, doi:10.1175/1520-0442(2000)013<0383:acsorc>2.0.co;2.
- 467 Medeiros, B., C. Deser, R. A. Tomas, and J. E. Kay (2011), Arctic Inversion Strength in Climate
468 Models, *Journal of Climate*, 24(17), 4733-4740, doi:10.1175/2011jcli3968.1.
- 469 Meng, Q., Y. Zhang, and M. Xu (2017), Viability of transarctic shipping routes: a literature
470 review from the navigational and commercial perspectives, *Maritime Policy & Management*,
471 44(1), 16-41, doi:10.1080/03088839.2016.1231428.
- 472 Miller, L. B., J. C. Hallo, R. G. Dvorak, J. P. Fefer, B. A. Peterson, and M. T. J. Brownlee
473 (2020), On the edge of the world: examining pro-environmental outcomes of last chance tourism
474 in Kaktovik, Alaska, *Journal of Sustainable Tourism*, 1-20,
475 doi:10.1080/09669582.2020.1720696.
- 476 Ng, A. K. Y., J. Andrews, D. Babb, Y. Lin, and A. Becker (2018), Implications of climate
477 change for shipping: Opening the Arctic seas, *WIREs Climate Change*, 9(2), e507,
478 doi:10.1002/wcc.507.
- 479 O'Neill, B. C., et al. (2016), The Scenario Model Intercomparison Project (ScenarioMIP) for
480 CMIP6, *Geosci. Model Dev.*, 9(9), 3461-3482, doi:10.5194/gmd-9-3461-2016.

- 481 O'Neill, B. C., E. Kriegler, K. Riahi, K. L. Ebi, S. Hallegatte, T. R. Carter, R. Mathur, and D. P.
482 van Vuuren (2014), A new scenario framework for climate change research: the concept of
483 shared socioeconomic pathways, *Climatic Change*, *122*(3), 387-400, doi:10.1007/s10584-013-
484 0905-2.
- 485 Ødemark, K., S. B. Dalsøren, B. H. Samset, T. K. Berntsen, J. S. Fuglestedt, and G. Myhre
486 (2012), Short-lived climate forcers from current shipping and petroleum activities in the Arctic,
487 *Atmos. Chem. Phys.*, *12*(4), 1979-1993, doi:10.5194/acp-12-1979-2012.
- 488 Overland, J. E., J. A. Francis, E. Hanna, and M. Wang (2012), The recent shift in early summer
489 Arctic atmospheric circulation, *Geophysical Research Letters*, *39*(19),
490 doi:10.1029/2012gl053268.
- 491 Parkinson, C. L., and D. J. Cavalieri (2008), Arctic sea ice variability and trends, 1979–2006,
492 *Journal of Geophysical Research: Oceans*, *113*(C7), doi:10.1029/2007jc004558.
- 493 Peters, G. P., T. B. Nilssen, L. Lindholt, M. S. Eide, S. Glomsrød, L. I. Eide, and J. S.
494 Fuglestedt (2011), Future emissions from shipping and petroleum activities in the Arctic,
495 *Atmos. Chem. Phys.*, *11*(11), 5305-5320, doi:10.5194/acp-11-5305-2011.
- 496 Ramanathan, V., and G. Carmichael (2008), Global and regional climate changes due to black
497 carbon, *Nature Geoscience*, *1*(4), 221-227, doi:10.1038/ngeo156.
- 498 Rigor, I. G., J. M. Wallace, and R. L. Colony (2002), Response of Sea Ice to the Arctic
499 Oscillation, *Journal of Climate*, *15*(18), 2648-2663, doi:10.1175/1520-
500 0442(2002)015<2648:rositt>2.0.co;2.
- 501 Ryan, J. C., A. Hubbard, M. Stibal, T. D. Irvine-Fynn, J. Cook, L. C. Smith, K. Cameron, and J.
502 Box (2018), Dark zone of the Greenland Ice Sheet controlled by distributed biologically-active
503 impurities, *Nature Communications*, *9*(1), 1065, doi:10.1038/s41467-018-03353-2.
- 504 Sand, M., T. K. Berntsen, J. E. Kay, J. F. Lamarque, Ø. Seland, and A. Kirkevåg (2013a), The
505 Arctic response to remote and local forcing of black carbon, *Atmos. Chem. Phys.*, *13*(1), 211-
506 224, doi:10.5194/acp-13-211-2013.
- 507 Sand, M., T. K. Berntsen, Ø. Seland, and J. E. Kristjánsson (2013b), Arctic surface temperature
508 change to emissions of black carbon within Arctic or midlatitudes, *Journal of Geophysical
509 Research: Atmospheres*, *118*(14), 7788-7798, doi:10.1002/jgrd.50613.
- 510 Sand, M., T. K. Berntsen, K. von Salzen, M. G. Flanner, J. Langner, and D. G. Victor (2016),
511 Response of Arctic temperature to changes in emissions of short-lived climate forcers, *Nature
512 Climate Change*, *6*(3), 286-289, doi:10.1038/nclimate2880.
- 513 Shindell, D. T., et al. (2008), A multi-model assessment of pollution transport to the Arctic,
514 *Atmos. Chem. Phys.*, *8*(17), 5353-5372, doi:10.5194/acp-8-5353-2008.
- 515 Stephenson, S. R., W. Wang, C. S. Zender, H. Wang, S. J. Davis, and P. J. Rasch (2018),
516 Climatic Responses to Future Trans-Arctic Shipping, *Geophysical Research Letters*, *45*(18),
517 9898-9908, doi:10.1029/2018gl078969.
- 518 Stewart, E. J., S. E. L. Howell, D. Draper, J. Yackel, and A. Tivy (2007), Sea Ice in Canada's
519 Arctic: Implications for Cruise Tourism, *Arctic*, *60*(4), 370-380.

- 520 Theocharis, D., S. Pettit, V. S. Rodrigues, and J. Haider (2018), Arctic shipping: A systematic
521 literature review of comparative studies, *Journal of Transport Geography*, *69*, 112-128,
522 doi:<https://doi.org/10.1016/j.jtrangeo.2018.04.010>.
- 523 von Schneidemesser, E., et al. (2015), Chemistry and the Linkages between Air Quality and
524 Climate Change, *Chemical Reviews*, *115*(10), 3856-3897, doi:10.1021/acs.chemrev.5b00089.
- 525 Wang, J., J. Zhang, E. Watanabe, M. Ikeda, K. Mizobata, J. E. Walsh, X. Bai, and B. Wu (2009),
526 Is the Dipole Anomaly a major driver to record lows in Arctic summer sea ice extent?,
527 *Geophysical Research Letters*, *36*(5), doi:10.1029/2008gl036706.
- 528 Warren, S. G. (1982), Optical properties of snow, *Reviews of Geophysics*, *20*(1), 67-89,
529 doi:10.1029/RG020i001p00067.
- 530 Watanabe, E., J. Wang, A. Sumi, and H. Hasumi (2006), Arctic dipole anomaly and its
531 contribution to sea ice export from the Arctic Ocean in the 20th century, *Geophysical Research*
532 *Letters*, *33*(23), doi:10.1029/2006gl028112.
- 533 Wu, D., Q. Li, X. Ding, J. Sun, D. Li, H. Fu, M. Teich, X. Ye, and J. Chen (2018), Primary
534 Particulate Matter Emitted from Heavy Fuel and Diesel Oil Combustion in a Typical Container
535 Ship: Characteristics and Toxicity, *Environmental Science & Technology*, *52*(21), 12943-12951,
536 doi:10.1021/acs.est.8b04471.
- 537
- 538
- 539

540

541 **Table 1.** Arctic wide average linear trend, per decade, 2035-2065, showing results from the
542 control simulation, the ensemble mean and the standard deviation of the ensemble.

543 **Figure 1.** Global maps of BC anthropogenic emissions in February 2050 for (a) the standard
544 SSP5-8.5 scenario forcing, (b) our modified forcing for the control simulation and (c) the
545 emissions associated with the “big kick” ensemble.

546 **Figure 2.** Time series of ice volume difference between the “big kick” ensemble mean and the
547 control simulation over the Arctic, expressed as a Z-score.

548 **Figure 3.** Response of BC in the Arctic and each subregion as defined by Parkinson and
549 Cavalieri [2008] showing (a) the feedback gain parameter of the CESM1-LENS ensemble
550 members selected pairwise (and a thumbnail map of the regions), and (b) a comparison between
551 the CESM1-LENS ensemble members and the experiments. Shading of the CESM1-LENS
552 results indicates the frequency of feedback gain value inferred from the probability density
553 function, with darker colors implying higher frequency. The boxplot displays the median (white
554 line) and interquartile range across four ensemble members of the “big kick” experiment.

555 **Figure 4.** Difference of sea level pressure between “big kick” ensemble mean and control for
556 each season, defined by the months indicated, for the period 2035-2065.

557 **Figure 5.** Relative change in spring ice volume between “big kick” ensemble member 1 and
558 control 2035-2065 by (a) total (b) dynamic (c) ridged and (d) thermodynamic processes. The
559 relative change is computed using $(\text{Value}_{\text{“big kick”}} - \text{Value}_{\text{control}}) / \text{Value}_{\text{control}}$.
560

561
562

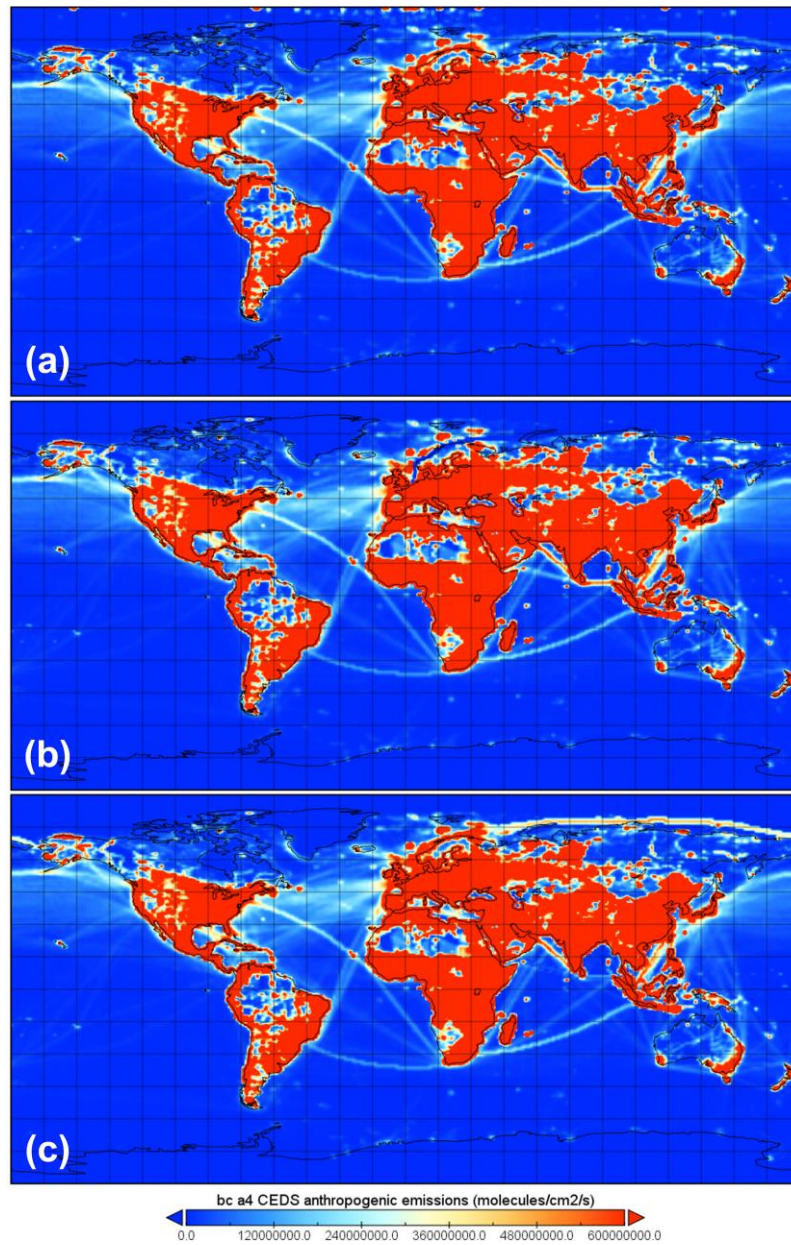
		Season			
		DJF	MAM	JJA	SON
Ice volume	Control	-0.008	-0.008	-0.008	-0.004
	“Big Kick”	-0.010 (0.003)	-0.009 (0.002)	-0.008 (0.002)	-0.005 (0.001)
Ice area	Control	-0.297	-0.106	-0.373	-0.515
	“Big Kick”	-0.358 (0.140)	-0.075 (0.070)	-0.383 (0.110)	-0.559 (0.119)
Albedo	Control	-0.001	0	0	-0.001
	“Big Kick”	-0.001 (0)	0 (0.0005)	0 (0)	0 (0.0005)
Surface temperature	Control	0.125	0.052	0.041	0.085
	“Big Kick”	0.156 (0.049)	0.058 (0.020)	0.043 (0.009)	0.088 (0.020)

563

564

565

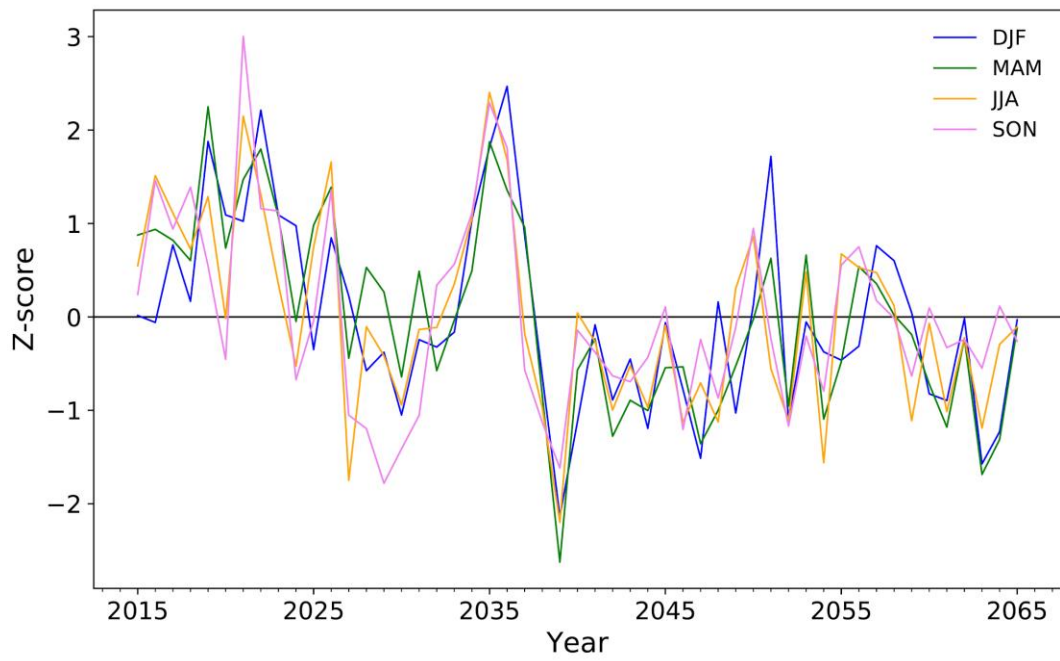
Table 1.



566
567

568
569

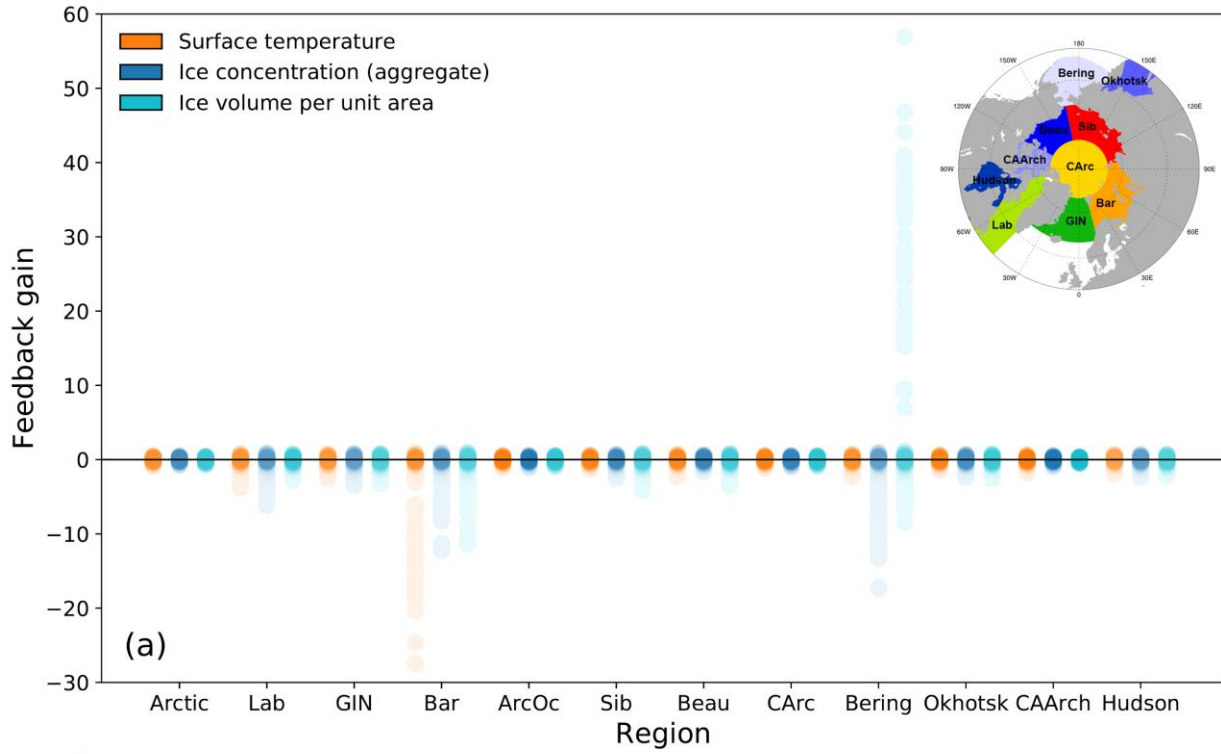
Figure 1.



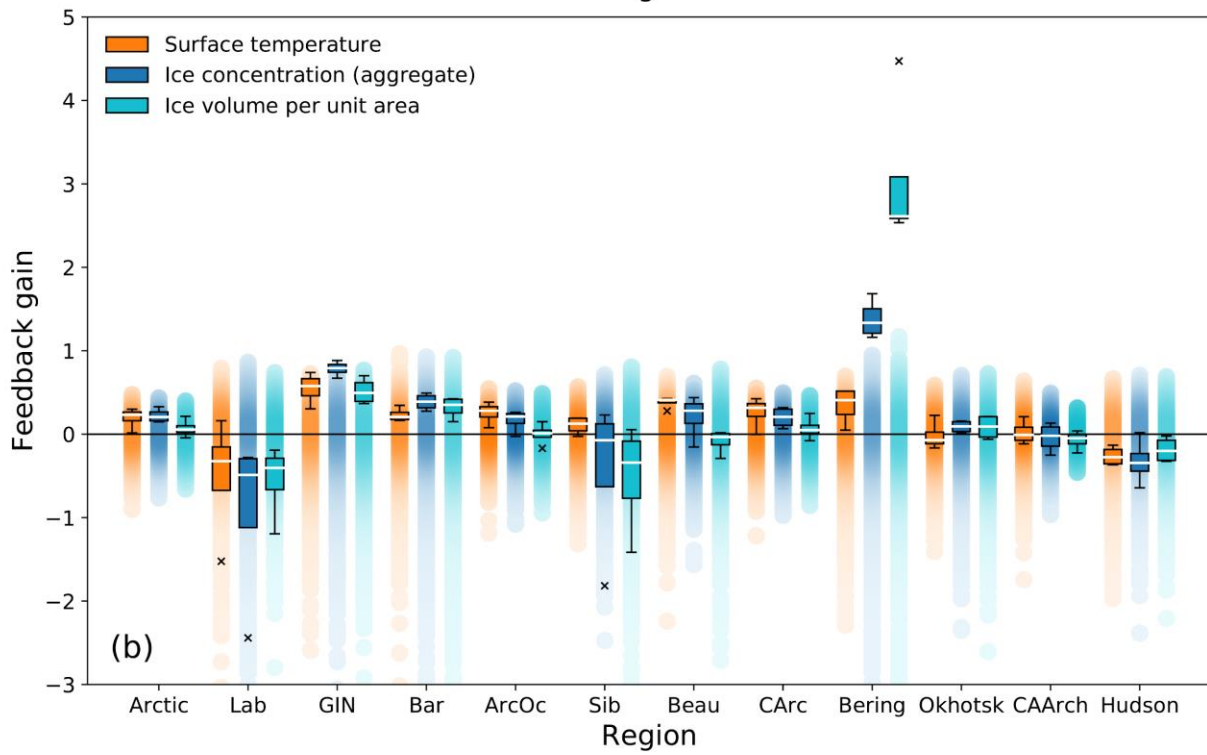
570
571

572
573

Figure 2.



574



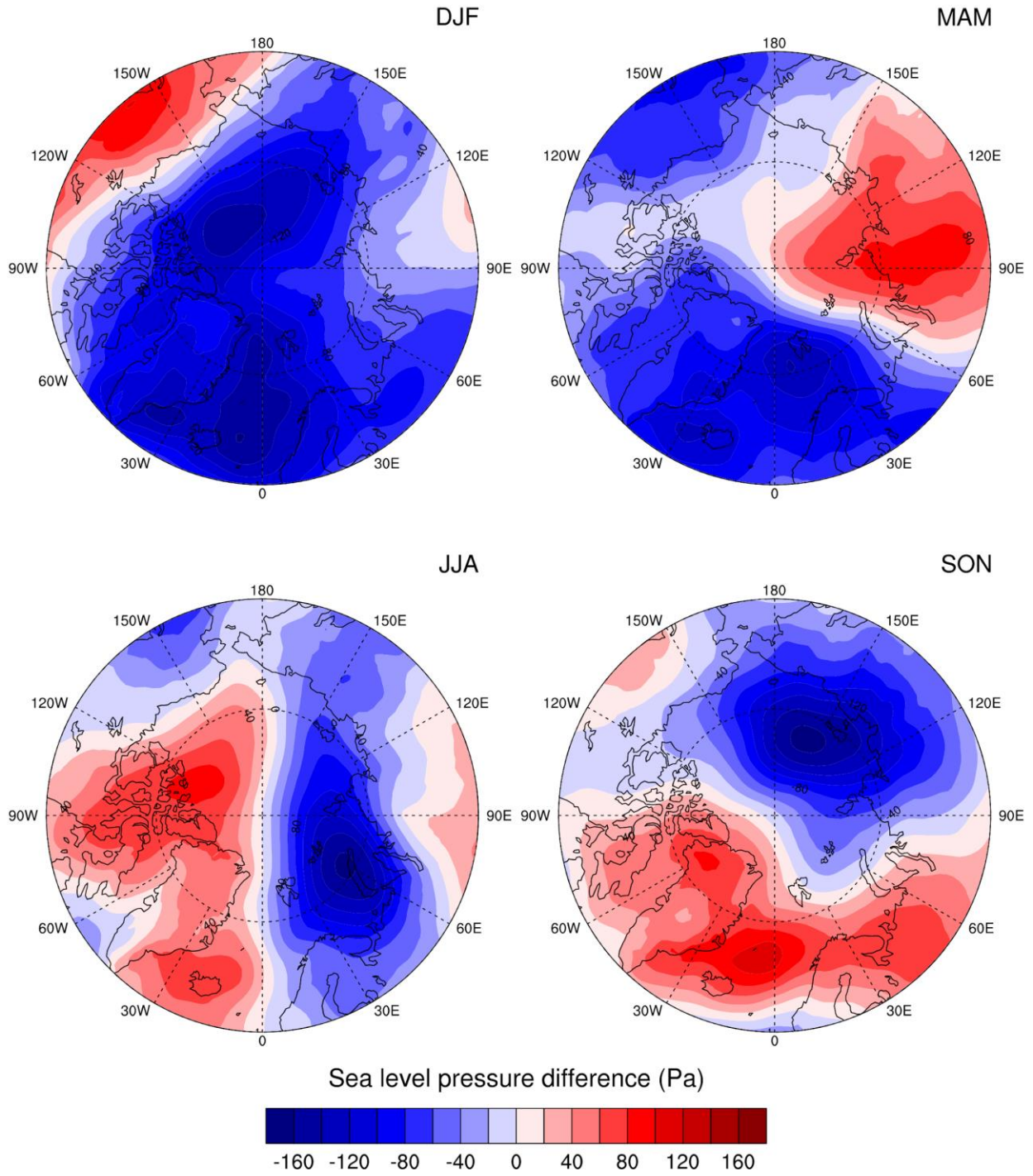
575

576

577

578

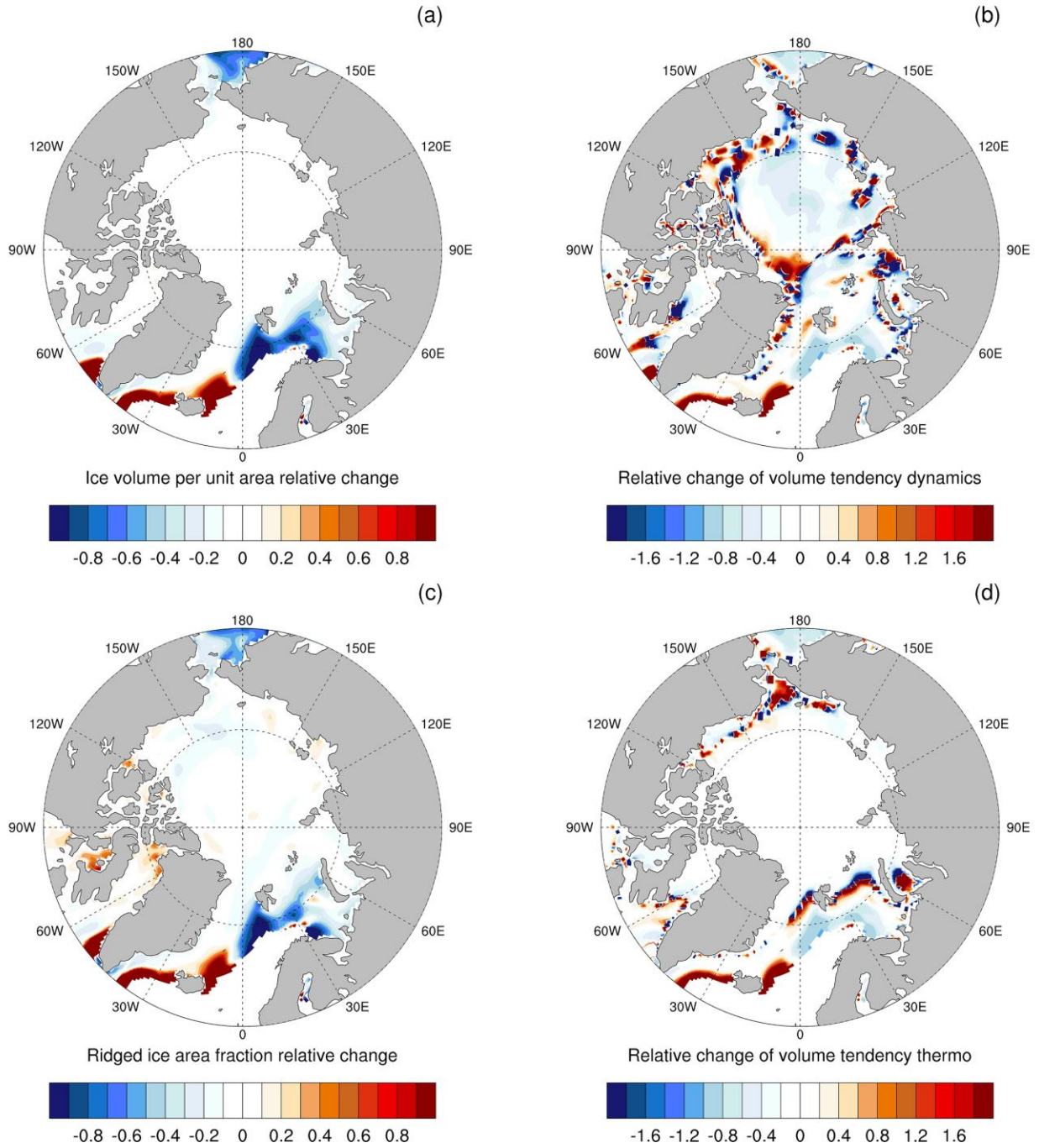
Figure 3.



579
580

581
582

Figure 4.



583
584

585

586

Figure 5.